RESEARCH ARTICLE

Editorial Process: Submission:04/25/2023 Acceptance:07/08/2023

The Effects of Umbilical Cord Mesenchymal Stem Cells -Derived Exosomes in Oral Squamous Cell Carcinoma *(In vitro* Study)

Amira Abdelwhab[1], Yasmine Alaa El-Din[2]*, Dina Sabry[3,4], Reham Lotfy Aggour[1]

Abstract

Objective: Mesenchymal stem cells (MSCs) derived exosomes offers several advantages as a cell-free therapeutic agents. In this study, Umbilical cord mesenchymal stem cells exosomes (UC-MSCs-exos) effects on oral squamous cell carcinoma (OSCC) cell line was evaluated. **Methods:** UC-MSCs-exos were isolated and co-cultured with OSCC cells and their impact on OSCC was explored by various tests. Comet assay and western blot for cleaved caspase-3 and immunocytochemistry for caspase-8 were used for apoptosis assessment. HO-1 and Nrf2 were used to determine antioxidant levels. Tumor necrosis factor-α and interleukin-6 were assessed as inflammatory biomarkers. HOX transcript antisense intergenic long noncoding RNA (HOTAIR) expression was also evaluated. **Results:** In a dose-dependent manner, UC-MSCs-exos reduced the levels of pro-inflammatory cytokines (IL-6 and TNF-α) and induced apoptosis of OSCC in vitro. Meanwhile, we found that UC-MSCs-exos downregulate HOTAIR. **Conclusion:** UC-MSCs-exos conferred a suppressive role on OSCC in vitro, highlighting a promising therapeutic role. However, the exact potentially involved molecules and molecular mechanisms need to be investigated in further studies.

Keywords: Umbilical cord mesenchymal stem cells- exosomes- HOTAIR- Oral squamous cell carcinoma- lncRNA

Asian Pac J Cancer Prev, **24 (7)**, 2531-2542

Introduction

Oral squamous cell carcinoma (OSCC) is one of the globally and a leading cause of mortality. Currently, the standard treatment modalities for OSCC are surgery, radiotherapy, and chemotherapy. Despite the multidisciplinary approaches, OSCC prognosis is still poor, especially after metastatic spread, and the overall survival rate within five years remains less than 50% (Zanoni et al., 2019). Therefore, the development of novel therapeutic modalities for treating OSCC is mandatory.

Umbilical cord mesenchymal stem cells (UC-MSCs) are characterized by self-renewal, multipotent capacity, and maintaining their stemness characteristics for extended periods (Gauthaman et al., 2011). Moreover, UC-MSCs are more primitive when compared with those obtained from other tissue sources. UC-MSCs does not express the primary histocompatibility complex class II antigens (less antigenicity) (Weiss et al., 2006) and are unlikely produce acute inflammatory reaction; therefore can potentially apply to humans without a complete genetic match (Weiss et al., 2008). Furthermore, a relatively massive number of MSCs can be harvested, separated, cultured, expanded, purified and stored without risk to the donor (Xie et al., 2020). UC-MSCs can inhibit the progression and initiation of hepatocellular carcinoma and cancer of the lung, indicating that UC-MSCs can exert tumor-suppressive effects (Yuan et al., 2018). Human UC-MSCs secrete exosomes during various biological processes and UC-MSCs-derived exosomes (UC-MSCs-exos) can act as a potential therapeutic agents (Kalluri, 2016, Zhang et al., 2016).

Exosomes are endosomal-derived vesicles of 50–100 nm and considered the main class of extracellular vesicles (EVs) that all cells can release. They deliver functional RNAs, proteins, and lipids from donor cells to recipient cells by direct fusion or active uptake (J O'Loughlin et al., 2012)). Exosomes' ability to transfer allows them to participate in various physiologic and pathological processes, including intracellular communication and regulation of immune response. (Zhang et al., 2014). Recently, exosomes have been developed as a promising cell-free modality for managing several diseases, including cancer (Katakowski et al., 2014). Exosomes are considered the key elements of paracrine signaling, which is regarded as the primary functional mechanism of MSCs (Armstrong et al., 2017). MSCs can produce a higher amount of exosomes (MSC-exos) when compared with other types of cells (Yeo et al., 2013). Additionally, using MSC-exos as cell-free therapeutics offers several advantages, when

*[1]Lecturer of Oral Medicine, Diagnosis and Periodontology, Faculty of Dentistry, October 6 University, Cairo, Egypt. [2]Lecturer of Oral and Maxillofacial Pathology, Faculty of Dentistry, October 6 University, Cairo, Egypt. [3]Department of Medical Biochemistry, Faculty of Medicine, Cairo University, Cairo, Egypt. [4]Department of Medical Biochemistry, Faculty of Medicine, Badr University in Cairo, Egypt. *For Correspondence: yasminealaaeldin.dent@o6u.edu.eg*

compared with their cellular counterparts, such as lower immunogenicity, higher stability, more accessible storage, and the ability to cross the blood-brain barrier (Yin et al., 2019).

According to the literature, MSC-derived exosomes can affect cancer growth, metastasis, and drug response in both suppressing and potentiating ways (Vakhshiteh et al., 2019). Zhao et al., (2018), reported that exosomes released from MSCs triggered the epithelial-mesenchymal transition (EMT) in lung cancer cells leading to tumor progression. Similar results were reported in another study (Dong et al., 2018). Malignant tumor progression and metastasis has also been demonstrated in breast cancer cells when treated with UC-MSCs-exos (Zhu et al., 2019). In contrary, Li et al., 2019, explored the role of engineered UC-MSCs-exos enriched with miR-302a in endometrial cancer. The data showed that miR-302a-loaded UC-MSCs-exos inhibited endometrial cancer cell proliferation and migration by suppressing the expression of cyclin D1 and the AKT signaling pathway. Because of these diverse effects, more studies, in different types of malignant neoplasms, is needed to elucidate the potential role of UC-MSCs-exos in cancer therapy.

Existing data has verified the pivotal part of long noncoding RNAs (lncRNAs) in the progression of OSCC by gene transcription regulation, epigenetic alterations, and posttranscriptional events. In particular, lncRNA and microRNA interference regulate OSCC metastasis via altering EMT (Han et al., 2020). Functional lncRNA differ from microRNA in that they can regulate gene expression at various levels, including chromatin modification, transcription, and posttranscriptional processes, which may impact EMT during cancer metastasis (Lei et al., 2021). The lncRNA expression profile in the human oral mucosa was first described by Gibb et al., (2011). They reported the expression of about 325 lncRNAs in the oral mucosa. Up to 60% of the detected lncRNAs were aberrantly expressed in premalignant lesions. They have shown that altered expression of lncRNAs can be used as diagnostic and prognostic biomarkers and potential therapeutic targets.

In OSCC, several lncRNAs showed differential expression. One of the most promising oncogenic long noncoding RNAs is the HOX transcript antisense intergenic RNA (HOTAIR). It is 2,158 base pairs long and works by silencing antisense (Chen et al., 2021). The effects of HOTAIR on colon, liver and pancreatic cancers have been well studied, indicating that it may directly regulate progression and be associated with cancer prognosis. Furthermore, the expression of HOTAIR was elevated in OSCC, and the higher expression levels were related to a poorer overall survival rate (Kolenda et al., 2017). HOTAIR overexpression was related to unfavorable prognosis and higher tumor stage and metastasis (Lu et al., 2017).

The effects of UC-MSCs-exos on OSCC is still unknown. Thus, in this study, we aimed to identify the biological effects of UC-MSCs-exos on OSCC, in vitro, including effect on HOTAIR expression level.

Materials and Methods

Culture of UC-MSCs

An umbilical cord sample was donated from the Obstetrics unit during cesarian section delivery after taking the mother's consent. UC-MSCs were isolated and propagated in a sterile tissue 50 cm^2 flask in a complete medium containing Dulbecco's modified Eagle's medium (DMEM) enriched with 10% fetal bovine serum and 100 U/mL penicillin and 100 µg/mL streptomycin (Gibco, Thermo Fisher, Scientific, Inc.) in 95% air and 5% CO_2 at 37°C. DMEM was replaced each 2-3 days to maintain the viability of cells. Trypsinization of cells with 0.25% trypsin-EDTA solution (Gibco, Thermo Fisher, Scientific, Inc was performed after reaching about 90% confluence, and then subculturing was held for continuous proliferation. Evaluation of the potential differentiation abilities of the UC-MSCs was done in the fourth passage as follows: UC-MSCs were cultured in StemPro® adipogenic differentiation kit (Gibco, Life Technology, Carlsbad, CA, USA) and then staining was performed using Alcian blue stain (Sigma- Aldrich, St Louis, MO, USA). Additionally, UC-MSCs were cultured in a StemPro® osteogenesis differentiation kit (Gibco, Life Technology) and stained by Alizarin Red Stain (Sigma-Aldrich) guided by the manufacturer's instructions for 21 days. Passages of UC-MSCs 5-8 culturing were done in DMEM medium-depleted phosphate-buffered saline (PBS). The culture supernatant was collected for further exosome isolation after 36-48 hours.

Isolation and identification of UC-MSCs exosomes

UC-MSC-exosomes were extracted and purified following a previous protocol (Sabry et al., 2019) from the supernatant by differential ultracentrifugation. Briefly, the steps started with centrifuging of the culture supernatant, which was held at 300×g for 10 min, 2,000×g for 10 min, and 10,000 ×g for 30 min at 4°C successively to remove dead cells and debris. After that, the exosome pellets were harvested at 100,000×g ultracentrifugation for 70 min at 4°C and resuspended with sterile PBS for another round of ultracentrifugation (Beckman Coulter Optima L-90K ultracentrifuge). In the end, suspension of the pellet of exosomes was done in 100 µl PBS and aliquoted for storage at -80°C. Lowry Protein Assay Kit (Bio Basic Inc. Canada) was used to assess the total protein concentration of exosomes according to the manufacturer's guide instructions. The exosomes's morphology and identification was detected by a transmission electron microscopy (TEM, HT-7700, Hitachi, Japan) and western blot using both CD-63 and CD-81.

Culture of OSCC

Human tongue oral SCC cell line (SCC-25) was the cell line that was used in the current experiment. It was purchased from VACSERA Holding company in Egypt. The cells were grown in DMEM with 10% bovine calf serum (Gibco BRL) and 1% PS (Penicillin-Streptomycin) at 37°C with 5% CO_2 in the air. In culture dishes, cells were seeded and cultured. OSCCs were gently washed, trypsinized, reseeded, and passaged every two to three

days once confluence reached 80–90%. The cell pellet was resuspended in fresh growth media. For further assays, the seeding of cells was in 6-well plates.

The groups of the present study were divided into eight groups; isolated and propagated UC-MSCs only, control untreated OSCC and six groups of OSCC treated with gradually increasing concentrations of UC-MSCs-exosomes (0.5, 1, 2, 3, 4, 5µg protein concentration) as shown in Table 1.

Assessment of cell apoptosis by comet assay

The comet assay was conducted under alkaline conditions with some modifications, as described by Singh et al. 1988). Apoptotic cell death is traditionally distinguished from other types of cell death by specific morphological and biochemical features. First, a 0.5% standard agarose layer was used to cover the microscope slides. Next, separated cells from various groups were washed using a washing buffer. The slides were then immediately covered with coverslips after a 50 µl aliquot of the cell sample, and 100 µl of 0.5% low melting point agarose was added. All slides were immersed in a lysing solution (2.5M NaCl, 100mM EDTA, ten mM Tris, NaOH to pH 10, 1% N-Lauryl Sarcosine, to which 1% Triton X-100 and 10% DMSO were freshly added at the beginning) for 1 hour at 4°C after the cover glass was removed. An electrophoresis tank was used for the placement of the slides which contains freshly prepared alkaline buffer (300 mM NaOH, 1 mM EDTA, pH > 13). The electrophoresis was conducted at room temperature for 20 min at 300 mA and 25 V. After that, the slides were washed three times for 5 min with neutralizing buffer (0.4 M Tris, pH 7.5). Later, washing with ethanol was performed for the same time and fixation in the buffer. Finally, staining of DNA with ethidium bromide was conducted (60 µl of a 20 µl/ml). DNA tail migration was analyzed with at least 75 randomly selected cells per sample by Comet Assay automatic image analysis system fitted with a Leica fluorescence microscope.

Antioxidant, proliferative and inflammatory markers assessment by ELISA

Cell supernatant was centrifuged for 20 minutes at 1000×g at 2-8°C to remove insoluble impurities and cell debris. Collection of the clear supernatant was done to carry out the assay immediately. Human HO-1 concentrations quantification (pg/ml) in cell culture supernatants was assessed using PicoKine™ ELISA (Cat. no: EK0888) according to manufacturer's instructions. For quantitative detection of Nrf2 (ng/ml) in cell culture supernatants, Fine Test Elisa Kit (Cat. no: EH3417) was applied according to the manufacturer's instructions. Inflammatory markers (IL-6, TNF-α) were assessed by ELISA KIT Cloud-Clone Cop. (Cat. No. SEA079Hu) and (cat. No: SEA133Hu), respectively according to the manufacturer's instructions. A range of 490 to 630 nm of OD, color absorbance was read using an Enzyme-Linked Immuno-Sorbent Assay (ELISA) plate reader (Stat Fax 2200, Awareness Technologies, Florida, USA). Using linear regression of each average relative OD against the standard curve produced by curve fitting software, the observed concentration in the samples was interpolated.

Assessment of HOTAIR expression by RT-PCR

Total RNA was extracted from cell pellets of all different groups using Direct-zol RNA Miniprep Plus (Cat# R2072, ZYMO RESEARCH CORP., USA). The amount and quality were then evaluated using a Beckman dual spectrophotometer (USA). Thermo Fisher Scientific, Waltham, Massachusetts, USA, supplied the SuperScript IV One-Step RT-PCR kit (Cat# 12594100) for reverse transcription and PCR of the isolated RNA. The following thermal profile was created using the step one equipment from Applied Biosystems, USA: Reverse transcription takes 10 minutes at 45 degrees, 2 minutes at 98 degrees, 40 cycles of 10 seconds at 98 degrees, 10 seconds at 55 degrees, and 30 seconds at 72 degrees for the amplification phase. The expression of data in Cycle threshold (Ct) for the target genes and housekeeping gene was performed after the RT-PCR. Normalization for expression variation of target genes; LncRNA HOTAIR was conducted regarding the mean critical threshold (CT) expression values of the GAPDH housekeeping gene by the ΔΔCt method. The relative quantitation (RQ) of each target gene was quantified according to the $2^{-\Delta\Delta Ct}$ method calculation. LncRNA HOTAIR gene sequence of its primers was forward 5′- GGGGCTTCCTTGCTCTTCTTATC-3′, and reverse 5`- GGTAGAAAAAGCAACCACGAAGC-3′, (gene bank accession number is NR_047518.1), and GAPDH housekeeping gene was forward 5'-CAATGACCCCTTCATTGACC-3' and reverse 5'-GACAAGCTTCCCGTTCTCAG -3' (gene bank accession number is DQ40057.1).

Apoptosis assessment by Western Blot

Western blot was applied for quantitative assessment of the Cleaved caspase-3 apoptotic protein marker. The Ready Prep TM protein extraction kit (total protein) was provided by Bio-Rad Inc (Catalog #163-2086) which was employed according to manufacturer guidelines. Bradford Protein Assay Kit (SK3041) was used to measure quantitative protein analysis (Bio basic Inc, Markham Ontario L3R 8T4 Canada). A similar volume of 2x Laemmli sample buffer containing 4% SDS, 10% 2-mercaptoethanol, 20% glycerol, 0.004% bromophenol blue, and 0.125 M Tris HCl was loaded onto 20 µg of protein from each sample. The TGX Stain-Free TM FastCast TM Acrylamide Kit (SDS-PAGE), made available by Bio-Rad Laboratories Inc. under catalogue number 161-0181which was used to create polyacrylamide gels. The gel was assembled in a 1x transfer buffer. Then, the blot was run for 7 min at 25 V to allow protein bands to transfer from gel to membrane using BioRad Trans-Blot Turbo. The primary antibody of cleaved caspase-3 (MERCK, Germany, catalogue number AB3623) was purchased and was diluted in TBST (1:500) according to manufactured instructions. Incubation was done overnight in each primary antibody solution, against the blotted target protein, at 4°C. At room temperature, incubation was performed in the HRP-conjugated secondary antibody (Goat anti-rabbit IgG- HRP-1mg Goat mab -Novus Biologicals) solution against the blotted target protein for 1 hr. The chemiluminescent substrate

was applied to the blot according to the manufacturer's recommendation (Clarity TM Western ECL substrate Bio-Rad cat#170-5060). Concisely, the same volumes were added from solution A (Clarity western luminal/ enhancer solution) and solution B (peroxidase solution). CCD camera-based imager was used for capturing the chemiluminescent signals. Reading the intensity of the band of the target proteins against the control sample beta-actin (housekeeping protein) was done using image analysis software which was used by protein normalization on the ChemiDoc MP imager.

Apoptosis assessment by immunocytochemistry

The technique of Immunocytochemistry was used to detect the immunopositivity of cells in the OSCC cells and effect of UC-MSD s exo. Seeding of the cells were done on a 96 well plate with glass bottom followed by fixation of the cells in 100% methanol/10 min at room temperature in addition to permeabilization with 0.25–0.5% Triton X-100 in PBS/10 min. Following this step, incubation for 24 h with caspase-8 antibody (1:500, Abcam, Cambridge, UK) was performed. Washing after the immunostaining step was done and anti-rabbit IgG (1:1000) as a secondary antibody was added for 1h. Finally, caspase-8 immuno-expression cells' percentage of was quantified in five images/each group using the Image-Pro Plus program.

Statistical analysis

The mean and standard deviation (SD) values were used to represent numerical data. The Shapiro-Wilk and Levene tests determined whether the variance was homogeneous and normal, respectively. One-way ANOVA was used to evaluate intergroup differences, and then Tukey's post hoc analysis was performed. For analysis, the Pearson correlation coefficient was utilized. At $p<0.05$, the significance level was established. R statistical analysis software for Windows (R Core Team (2022). R: A language and environment for statistical computing. R Foundation for Statistical Computing, Vienna, Austria. URL https://www.R-project.org/), version 4.1.3, was used to conduct the statistical analysis.

Results

The results of different techniques revealed significant difference between the groups. Apparently, the effectiveness of UC-MSCs exos on OSCC increased by increasing the concentration. Figure 1(a-f) revealed the difference between the nature of cells of all studied groups and differentiation of UC-MSCs into adipocytes, and osteocytes which was evaluated by using the inverted microscope.

Using transmission electron microscope (TEM), showed exosomes' ultrastructure as a spheroid and a well-defined membrane with heterogeneous contents. Their diameter was less than 100 nm, as shown in (figure 2-a). Moreover, exosomes expression using exosome markers CD-63 and CD-81 was shown in (Figure 2-b) as thicker bands for exosomes.

Table 1. Study Design Showing Symbols of the Groups

Groups	Symbol
UC-MSCs	UC-MSCs
OSCC	OSCC
UC-MSCs exos 0.5µg	A
UC-MSCs exos 1µg	B
UC-MSCs exos 2µg	C
UC-MSCs exos 3µg	D
UC-MSCs exos 4µg	E
UC-MSCs exos 5µg	F

Results obtained by Comet assay

Results of intergroup comparisons for Comet assay measurements were presented in Figures 3 and 4.

DNA tail length (µm)

Comet assays demonstrated a longer tail-DNA length reflecting increase in DNA damage in the OSCC cells after treatment with different concentrations of UC-MSCs exos. The results showed that UC-MSCs exos treatment induced DNA damage in OSCC cells in a dose-dependent manner thus accelerating apoptosis of OSCC cells. The results revealed a statistically significant difference between groups ($f=598.00$, $p<0.001$). The highest value

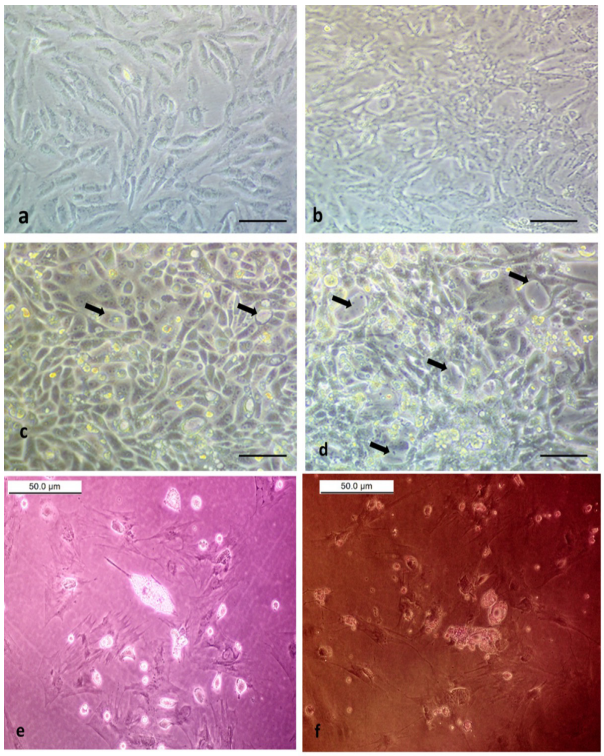

Figure 1. Phase Contrast Inverted Microscope Illustrated All Groups (Scale bar 10 nm): a- UC-MSCs (spindle fusiform shaped adhesive cells), b: OSCC, c: UC-MSCs exosomes (1µg) treated OSCC (black arrows for apoptotic cells) d: UC-MSCs exosomes (2µg) treated OSCC (black arrows for apoptotic cells), e: MSCs differentiated into adipocytes which was stained with Red Oil O (50µm), f: MSCs differentiated into osteocytes which was stained with Alizarin red (50µm).

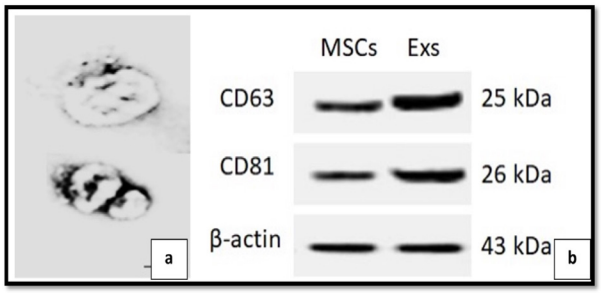

Figure 2. Photographs Showing Identification of Exosomes Using a: TEM picture for exosomes with ultrastructure magnification (scale bar was 200nm), b: Western blot detection using exosomes markers.

was for group (F) (15.26±0.53), followed by group (E) (11.27±0.02), then group (D) (7.77±0.86), group (C) (6.24±0.69), group (B) (2.98±0.17), group (A) (1.37±0.12) and OSCC (0.72±0.10), while the lowest value was found in UC-MSCs (0.68±0.11). Post hoc pairwise comparisons barley recorded a significant difference (no significance) between UC-MSCs, OSCC and group (A) ($p>0.05$). It was revealed that other groups had significant difference from each other ($p<0.001$). As shown in Figure 4 increased DNA tails in different UC-MSCs exo concentration.

Results obtained by ELISA assessment of antioxidant, proliferative and inflammatory markers

HO-1 (pg/ml)

As shown in Figure 5 (a), a significant difference between groups ($f=78.63$, $p<0.001$) was recorded. In a dose-dependent manner, the level of HO-1 (pg/ml) was obviously increased by UC-MSCs exos treatment compared with untreated OSCC group. The highest value was for group (E) (447.50±28.30), followed by group (F) (446.75±37.84), then group (D) (432.00±13.74), UC-MSCs (409.50±38.92), group (C) (366.50±39.52), group (B) (228.00±17.72) and group (A) (166.25±14.10), while the lowest for OSCC (130.00±33.50) group. Post hoc pairwise comparison showed that values for group (E) and (F) were significantly higher than OSCC and groups (A), (B) and (C) ($p<0.001$). In addition, values for

Table 2. Correlations between HOTAIR and Different Parameters

Parameters		r	p-value
lncRNA	DNA tail length (μm)	-0.62	<0.001*
(HOTAIR)	HO-1 (pg/ml)	-0.93	<0.001*
	Nrf2 (ng/ml)	-0.89	<0.001*
	IL-6 (pg/ml)	0.95	<0.001*
	TNF-α (pg/ml)	0.92	<0.001*
	Cleaved caspase-3	-0.63	<0.001*

UC-MSCs and groups (C) and (D) revealed significantly higher values than OSCC and groups (A) and (B) ($p<0.001$).

Nuclear factor erythroid 2-related factor 2 (Nrf2) (ng/ml)

Significant difference was exhibited between different groups ($f=62.20$, $p<0.001$). The highest value was for a group (F) (4.42±0.41), followed by group (E) (4.10±0.42), then group (D) (3.55±0.26), group (C) (2.98±0.30), UC-MSCs (2.95±0.39), group (B) (1.90±0.37) and group (A) (1.40±0.14), while the lowest value was for OSCC group (0.78±0.25). Post hoc pairwise comparison records revealed group (E) to be significantly higher than other groups except for group (D) ($p<0.001$). In addition, group (D) results showed highly significant values than other groups with lower mean values except for UC-MSCs and group (C) ($p<0.001$). Considering Group (C), results showed significantly higher values than other groups except for UC-MSCs ($p<0.001$), Figure 5 (b).

IL-6 (pg/ml)

A significant difference was presented between different groups ($f=43.48$, $p<0.001$). The highest value was found for OSCC (87.92±18.66), followed by group (A) (65.30±5.07), then group (B) (44.15±5.76), group (D) (26.50±3.41), group (C) (25.30±5.54), group (E) (21.15±2.45) and group (F) (20.55±2.40), while the lowest values were for UC-MSCs (15.70±5.28). Post hoc pairwise comparison records showed OSCC to be significantly higher than other groups ($p<0.001$). In addition, group

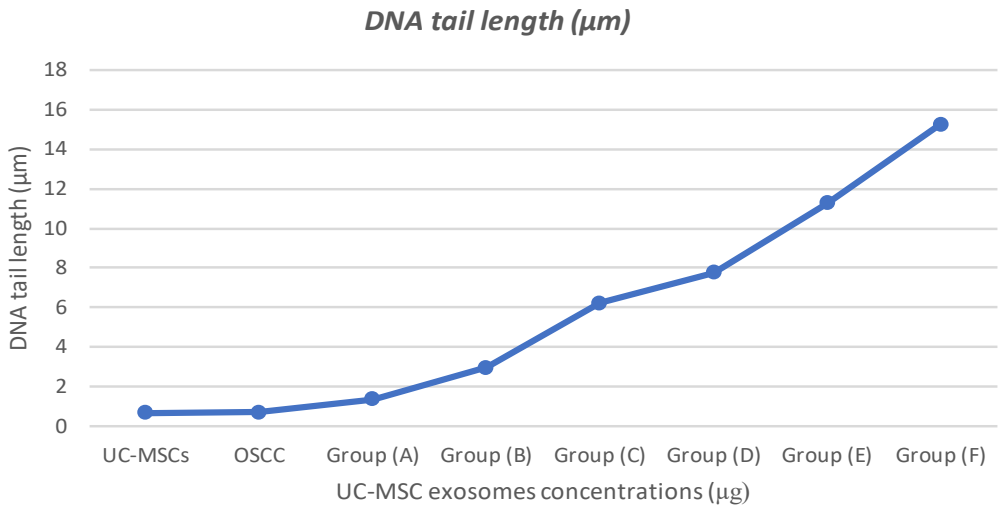

Figure 3. Line Chart Showing Mean Values for DNA Tail Length (μm)

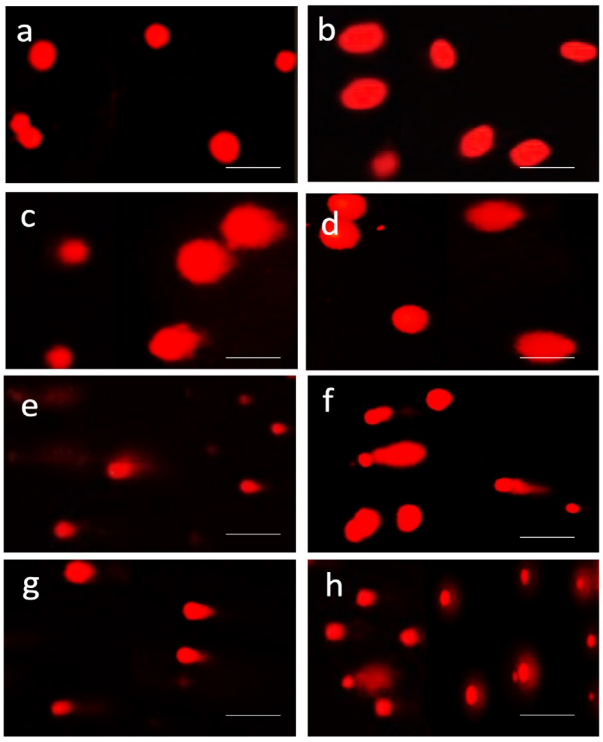

Figure 4. Comet Assay Analysis Figures (Scale bar 50nm) showing: a- UC-MSCs, b: OSCC, c: UC-MSCs exosomes (0.5µg) treated OSCCs, d: UC-MSCs exosomes (1µg) treated OSCC, e: UC-MSCs exosomes (2µg) treated OSCC, f: UC-MSCs exosomes (3µg) treated OSCC, g: UC-MSCs exosomes (4µg) treated OSCC, h: UC-MSCs exosomes (5µg) treated OSCC.

(A) showed a significantly higher value than other groups ($p<0.001$). Finally, it was revealed that group (B) to be a substantially higher value than other groups with lower mean values ($p<0.001$), Figure 5 (c).

TNF-α (pg/ml)

As shown in figure 5 (d), a significant difference between groups (($f=36.98$, $p<0.001$)) was recorded. In a dose-dependent manner, the level of TNF-α (pg/ml was obviously decreased by UC-MSCs exos treatment compared with untreated OSCC group. The highest value was for OSCC (22.52±4.87), followed by group (A) (18.42±2.35), then group (B) (13.60±1.67), group (C) (10.97±1.28), group (D) (7.97±0.66), group (E) (7.00±0.93) and group (F) (5.03±0.62), while the lowest values were for UC-MSCs (4.80±0.96). A highly significant difference was recorded by Post hoc pairwise comparisons which showed OSCC to be significantly higher than other groups except for group (A) ($p<0.001$). Regarding group (A), results showed significantly higher values than other groups except for group (B) ($p<0.001$). Group (B) showed a significantly higher value except for group (C) ($p<0.001$). Finally, group (C) was a significantly higher value than UC-MSCs and grup (F) ($p<0.001$).

Results obtained by assessment of HOTAIR expression by RT-PCR (Figure 6)

The recorded results showed a statistically significant difference between groups ($f=82.95$, $p<0.001$). A much higher expression level was reported for OSCC (4.66±0.62), followed by group (A) (3.85±0.41), then group (B) (2.76±0.36), group (C) (1.75±0.16), group (D) (1.38±0.09), group (E) (1.20±0.08) and group (F) (1.13±0.09), while the lowest value was for UC-MSCs (1.09±0.10). The Post hoc pairwise comparisons showed that HOTAIR expression in OSCC is significantly higher than other groups ($p<0.001$). HOTAIR expression decreased by increasing the concentration of UC-MSCs exos.

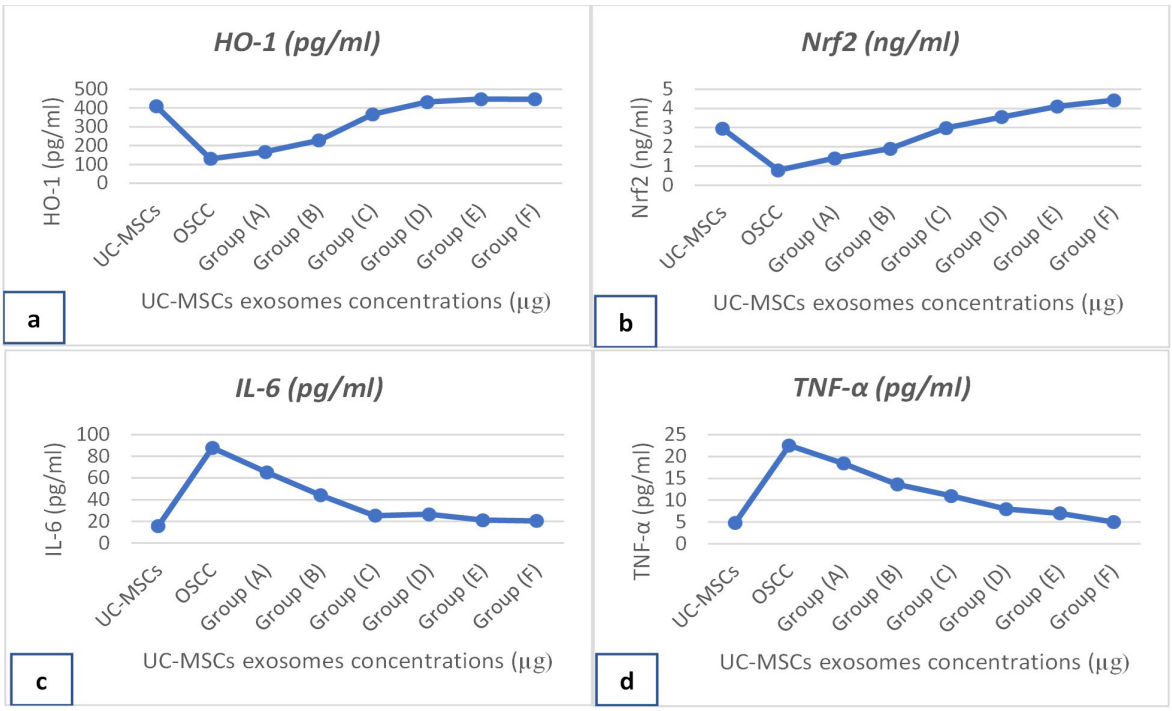

Figure 5. Line Chart Showing Mean Values of a: HO-1 (pg/ml), b: Nrf2 (ng/ml), c: IL-6 (pg/ml), d: TNF-α (pg/ml)

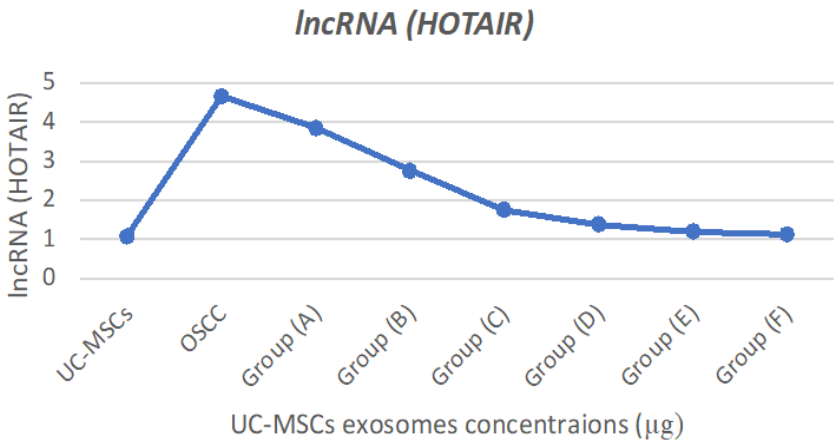

Figure 6. Line Chart Showing Mean Values for lncRNA (HOTAIR).

Western Blot (WB)

Results of intergroup comparisons for WB measurements were presented in Figure (7 a, b).

Cleaved caspase-3

WB was performed to confirm the involvement of caspase activity, since the activation of caspase pathways is usually involved in the apoptosis induction. In a dose dependent manner, the level of cleaved Caspase-3 significantly increased after treatment of OSCC cells with UC-MSCs-exos. A difference was significantly recorded between different groups (f=250.04, p<0.001). The highest value was for group (F) (5.50±0.33), followed by group (E) (4.11±0.18), then group (D) (3.90±0.12), group (C) (3.28±0.29), group (B) (2.35±0.17), group (A) (1.50±0.13) and UC-MSCs (1.02±0.18), while the lowest value was for OSCC (1.00±0.17). Post hoc pairwise comparisons results showed group (F) to be significantly higher than other groups (p<0.001).

Assessment of cell apoptosis by immunocytochemistry

Apoptotic cells were assessed also by using immunocytochemistry for caspase-8 as shown in Figure 8 (a-i). The present study revealed that treating OSCC cells by UC-MSCs exosomes significantly increased immunostaining incubation of immune-positive cells in a concentration-dependent manner when compared with the control untreated OSCC cells, (f=220.53, p<0.001). The highest value was found in group (F) (55.80±5.74), followed by group (E) (37.83±0.56), then group (D) (27.62±2.32), group (C) (18.32±2.96), group (B) (8.22±1.58) and group (A) (3.80±0.29), while the lowest value was found in OSCC (1.73±0.43). Post hoc pairwise comparisons showed group (F) to have significantly higher value than other groups (p<0.001). In addition, results showed group (E) to have significantly higher value than other groups with lower mean values (p<0.001). In addition, group (D) revealed significantly higher value than other groups with lower mean values (p<0.001) and group (C) recorded higher value than other groups with lower mean values (p<0.001). Finally, group (B) showed significantly higher value than OSCC (p<0.001), Figure (9).

Correlations between lncRNA (HOTAIR) and different parameters

Correlation between HOTAIR and different parameters showed a significant negative moderate correlation

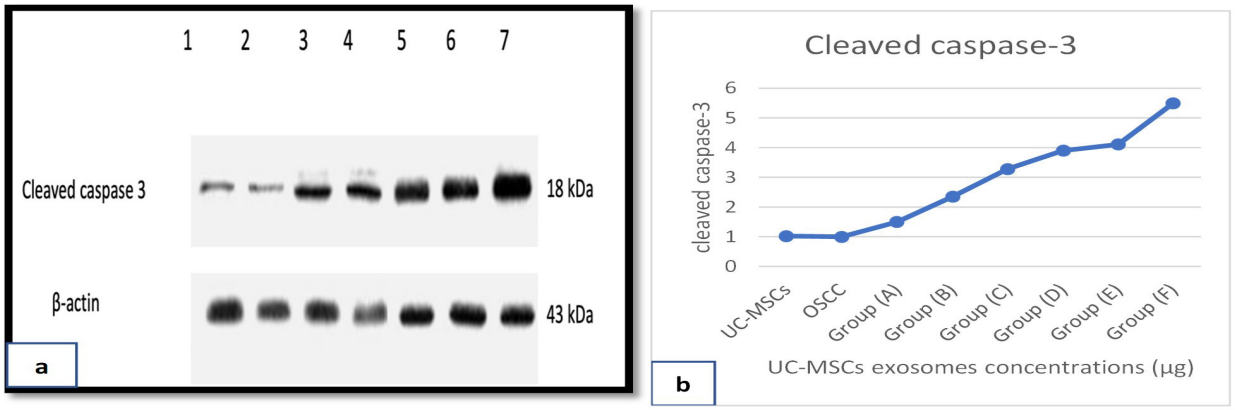

Figure 7. (a): Scanning densitometry picture for quantitative assessment bands of cleaved caspase-3 protein in all studied groups by western blot. Lane 1: OSCC, Lane 2: OSCC treated with UC-MSCs-exosomes (0.5µg), Lane 3: OSCC treated with UC-MSCs -exosomes (1µg). Lane 4: OSCC treated with UC-MSCs -exosomes (2µg). Lane 5: OSCC treated with UC-MSCs -exosomes (3µg). Lane 6: OSCC treated with UC-MSCs -exosomes (4µg). Lane7: OSCC treated with UC-MSCs -exosomes (5µg). (b): line chart showing mean values for Cleaved caspase-3.

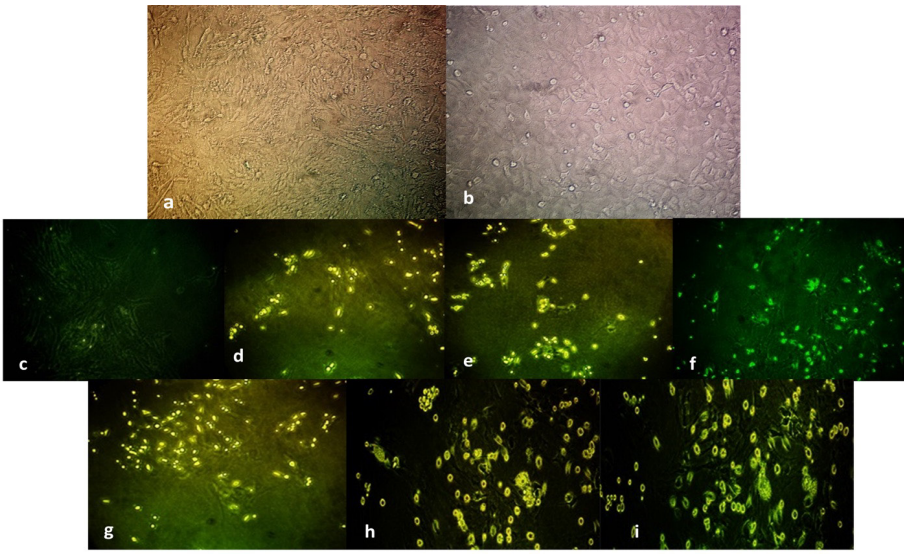

Figure 8. Phase Contrast Inverted Microscope Figure Illustrated All Groups (Scale bar 100μm): a: UC-MSCs (spindle fusiform shaped adhesive cells), b: OSCC (Cuboidal shaped adhesive cells. Immunocytochemistry for assessment of caspase-8 showed apoptotic cells with green fluorescence for OSCC treated with different concentrations of UC-MSCs exosomes, c: Control OSCC, d: (0.5μg), e: (1μg), f: (2μg), g: (3μg), h: (4μg), i: (5μg).

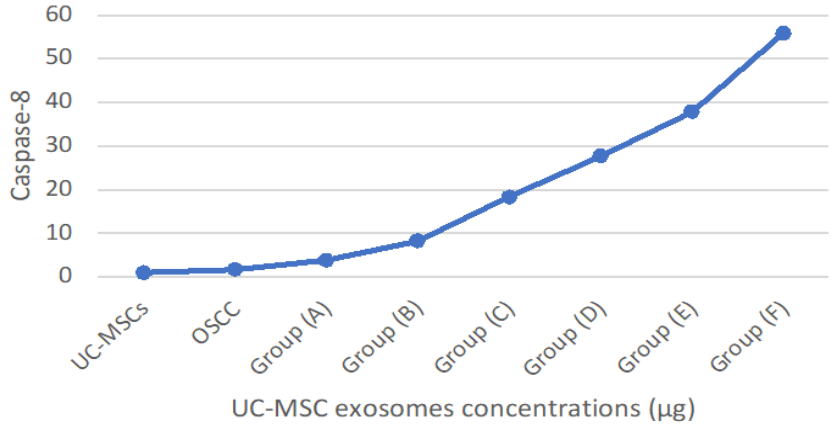

Figure 9. Line Chart Showing Mean Values for Caspase 8

between (HOTAIR -DNA tail length) and (HOTAIR - Cleaved caspase-3). Additionally, there was a significant negative correlation between (HOTAIR - HO-1) and (HOTAIR -Nrf2). In addition, a significant strong positive correlation between (HOTAIR - IL-6) and (HOTAIR - TNF-α) was recorded. Correlations between HOTAIR and different parameters were presented in Table 2.

Discussion

Globally, OSCC is characterized by progressive local invasion and significant regional lymph node metastases, increasing mortality, and a poor prognosis (Coyte et al., 2014). Chemotherapy, radiotherapy, and surgical removal of tumors are the principal approaches to increase survival rate (Tang et al., 2018). Although, the results of various treatment modalities for OSCC have recently improved, the 5-year survival rate was about 50%. Improvements in inhibition, early detection, and treatment effectiveness are urgently needed to reduce the risk of OSCC's adverse effects (Lu et al., 2021). Therefore, new approaches for targeted tumor therapy are being broadly studied. Studies for the therapeutic applications of UC-MSCs in different conditions including cancer have introduced UC-MSCs as an effective treatment (Zamani et al., 2022). Therefore, in this experiment, we studied the anti-cancer ability of UC-MSCs on OSCC cells. According to our knowledge, the current experiment is the first to evaluate the effect of UC-MSCs-exos on OSCC and it shed the light on the correlation between lncRNA HOTAIR expression and different parameters. This study showed that UC-MSCs-exos could elicit OSCC suppression and we speculate that their suppressive effect might be closely associated with suppressing HOTAIR expression. However, we cannot exclude the potential contributions of other contents from UC-MSCs-exos, which needs to be further investigated in the future studies.

In the current study, the impact of UC-MSCs-exos on OSCC was explored by various tests. Results of apoptosis assessment by Comet assay revealed a significant intergroup difference in DNA tail length (μm). The highest value was found in OSCC treated with UC-MSCs exos

5µg pt conc. Western blot was applied for quantitative assessment of cleaved caspase-3 apoptotic protein marker. Similarly, there was a significant difference between groups. The highest cleaved caspase-3 value was found in OSCC treated with UC-MSCs exos 5µg pt conc while the lowest value was found in OSCC. Regarding HO-1 and Nrf2, the levels (pg/ml) were apparently increased by UC-MSCs exos treatment compared with untreated OSCC group. In addition, in a dose-dependent manner, the levels of IL-6 and TNF-α and (pg/ml) were obviously decreased by UC-MSCs exos treatment compared with untreated OSCC group.

EVs are nano-sized, lipid-bilayer vesicles that are naturally discharged by cells into the extracellular matrix (ECM) (Thery et al., 2018). The three EV types are exosomes, microvesicles, and apoptotic bodies (Thery et al., 2018). Noncoding RNAs (ncRNAs), mRNAs, proteins, and DNA fragments have all been found to be transported as "cargo" in EVs and may serve as potential diagnostic biomarkers for OSCC (Jabbari et al., 2020, Ahmadi& Rezaie, 2020, Pourhanifeh et al., 2020). The exosome's cell origin determines its composition, bioactive behavior and targeting abilities into recipient cells. Notably, MSCs can produce exosomes interacting with various recipient cells to change a range of target cells' biological characteristics. Additionally, it can control the development of illnesses and physiologic homeostasis (Liew et al., 2017). In a mouse model for head and neck squamous cell carcinoma, Cohen et al., (2021), reported higher tumor accumulation and ability to penetrate the tumor and distribution throughout its tissue and cytoplasm of MSC-derived exosomes (MSC-exo) as compared to exosomes from the A431 human epidermal carcinoma cell line (A431-exo). The authors suggested that MSC-exo may have superior abilities for tumor-targeted therapy.

Exosomes exhibit prominent roles in controlling cellular activities during physiological and pathological conditions. They enable effective cell-to-cell communication and migration to sites of disease, transmitting proteins and nucleotides between cells and taking part in the intricate pathophysiology of tumor growth and metastasis (Weng et al., 2021). In cancer therapy, exosomes may have significant advantages over their cellular counterparts due to their lower immunogenicity and higher safety (He et al., 2020). MSC-derived exosomes have been exploited as an innovative therapeutic strategy in antitumor management (Qiu et al., 2020). Specifically, exosomes released by UC-MSCs can inhibit cell proliferation, invasion, migration, and apoptosis of malignant tumors, such as esophageal squamous cell carcinoma, ovarian cancer, and breast cancer (Yuan et al., 2019).

The malignant growth of OSCC has been linked to several pathways, but most studies focused on protein-coding genes rather than noncoding RNA (ncRNA) (Wu et al., 2014, Wu and Xie, 2015). The human genome only contains 2% protein-coding genes; most transcripts are noncoding RNAs, including (lncRNAs). Interestingly, lncRNAs are essential regulators of cellular functions like differentiation, proliferation, and metastasis (Wu et al., 2015). As a result, it is crucial to learn about lncRNA and its relationship to OSCC. Importantly, in this study, we screened the differentially expressed LncRNA HOTAIR between OSCC with or without UC-MSCs exo treatment. Results revealed a statistically significant difference between groups ($f=82.95$, $p<0.001$). A much higher expression level was reported for OSCC, which decreased by UC-MSCs exo treatment in a dose dependent manner.

HOTAIR is one of the lncRNA which performs as a tumor suppressor via sponging miR-148a in head and neck tumors (Yuan et al., 2019). In agreement with the study by (Wu et al., 2014, Wu et al., 2015), we demonstrated the effects of UC-MSCs-exos on the suppression of HOTAIR in OSCC cells. Wu et al., 2014, suggested UC-MSCs-exos targeted HOTAIR by inhibiting proliferation of cells and tumorgenicity (Wu et al., 2014). The precise molecular mechanisms underlying the HOTAIR targeting effects of UC-MSCs-exos may be variant in different types of cancers. Further investigation is needed to clarify the mechanisms of action. In line with the current study, results of Wu et al., (2014), Wu et al., (2015) and Wu et al., (2015), reported upregulation of HOTAIR expression in OSCC, which was suppressed in this present study by UC-MSCs exos treatment.

Our findings are in good agreement with previous Logan et al., (2013) and Nishiyama et al., (2018) research's findings. They claimed that the apoptosis rate and caspase-3 expressions was accelerated in OSCC cells after HOTAIR was silenced. Enhanced caspases activity could be a putative mechanism exerted by exosomes causing OSCC apoptosis. In the current study, correlation between HOTAIR and different parameters showed a significant negative moderate correlation between HOTAIR -DNA tail length and HOTAIR - cleaved caspase-3.

We further found that UC-MSCs-exos treatment significantly reduced the levels of IL-6 in a dose-dependent manner. IL-6 plays a crucial function in several "hallmarks" of tumorigenesis, inducing angiogenesis and sustaining proliferative signaling of solid cancers. Thereby, dysregulation of IL-6 signaling endorses cancer cell multiplying and survival intrinsically. Moreover, IL-6 supports tumor growth via activating angiogenetic factors extrinsically. Uz et al., (2019) proved a strong correlation between IL-6 and OSCC. Shinagawa et al., (2017), reported several effects of IL-6 in cases of cancer and inflammation, which regulates immunity and correlated with aggressive and invasive tumor types. Still, to our knowledge, the present study is the first to elucidate the effect of UC-MSCs-exos on IL-6 and TNF-α in OSCC, reflecting its role in reduction of the inflammatory response in OSCC. Knowledge over the active components of UC-MSC-exos is still partial, but its immunomodulatory effects appear to be relevant to the therapeutic impact. The restoration of tissue homeostasis via extracellular adenosine signaling may contribute to the immunomodulatory activity of exosomes by the conversion of AMP to adenosine by the GPI-anchored 5′-ecto-nucleotidase CD73 present on enriched UC-MSC EVs (Wu et al., 2014). Several studies had already revealed that UC-MSCs-exos could markedly influence the anti-inflammatory response by secreting great amounts of anti-inflammatory growth factors,

including epidermal growth factor, fibroblast growth factor, hepatocyte growth factor, and vascular endothelial growth factor (Cahill et al., 2016, Xiang et al., 2020, Li et al., 2016, Priglinger et al., 2021).

Undoubtedly, Oxidative stress plays an essential role in the development of OSCC. One of the cores of cellular defense mechanisms against oxidative stress is (Nrf2)–Kelch-like ECH-associated protein 1 (Keap1) signaling pathway which is believed to be under basal conditions. Nrf2 is sequestered in the cytoplasm by its repressor Keap1 and constitutively degraded through the ubiquitin-proteasome pathway. Nrf2 has dual roles in cancer development; on one hand, prevention of malignant transformation of normal cells. On the other hand, it encourages the survival of cancer cells (Matsouka et al., 2022, Zhou et al., 2013).

Heme oxygenase-1 (HO-1) is a 32-kDa microsomal enzyme that plays a crucial protective role in tissues and contributes to maintain cellular homeostasis. This is done by reducing oxidative damage and the inflammatory response induced by several factors, such as heme, oxidative stress, heavy metals, and inflammatory cytokines, among others (Costa et al., 2020). The current study's findings were like those of a prior investigation on HO-1's high expression in OSCC (Lee et al., 2008). Evidence indicates a role for HO protein in cellular or tissue damage and suggests that induction of HO-1 is a protective response against oxidative stress. In the current study, the level of HO-1 (pg/ml) was obviously increased by UC-MSCs exos treatment compared with untreated OSCC group with a significant negative correlation between it and HOTAIR expression.

In addition to anti-inflammatory effects, OSCC treated with UC-MSCs-exos demonstrated a longer tail-DNA length and a highly significant increase in DNA damage compared to the untreated OSCC cells. The current findings suggest that UC-MSCs-exos significantly induce the apoptosis of OSCC in vitro.

In conclusion, this study revealed that UCMSCs-exos could exert suppressing effects on OSCC. Limited studies have been conducted to investigate the role of UC-MSCs and none shed light on the effect of UC-MSCS-exos on inflammatory components, oxidative pathway, apoptosis, and correlation with lncRNA expression level. Furthermore, our results pave the way for further in vivo and preclinical experiments to investigate the clinical efficiency in the field of oral cancer.

Limitations

Although our study produced many insights, it still had limitations. Firstly, exosomes' structure contains many RNAs and proteins. In the present study, we did not clearly illuminate the specific biological factors that mediate exosomes effects on cancer cells, accordingly we should further explore these specific mediators in future studies. Another certain limitation of this study was inavailability of studying Knockout or overexpression of Lnc-HOTAIR which should be included in future experiments. Moreover, Clonal formation and migration ability of OSCCs with tumorigenesis tests in vivo experiments should be done to confirm the current study observations.

Recommendations

The present findings are encouraging for the evolution of animal studies for investigating the effect of UCMSC-exos on OSCC and correlation with HOTAIR expression.

List of abbreviations

MSCs: Mesenchymal stem cells

UC-MSCs- exos: Umbilical cord mesenchymal stem cells exosomes

HO-1: Heme oxygenase-1

Nrf2: nuclear factor erythroid2 -related factor2

HOTAIR: HOX transcript antisense intergenic RNA

nm: nanometre

lncRNAs: long noncoding RNAs

OSCC: Oral Squamous Cell Carcinoma

DMEM: Dulbecco's modified Eagle's medium

SCC: SCC cell line

ELISA: Enzyme-Linked Immuno-Sorbent Assay

Ct: Cycle threshold

RT-PCR: real time reverse transcription polymerase chain reaction

GAPDH: Glyceraldehyde3- phosphate dehydrogenase

SD: standard deviation

TEM: Transmission Electron Microscope

WB: Western Blot

Evs: Extracellular vesicles

ncRNAs: Noncoding RNAs

Keap1: Kelch-like ECH-associated protein 1

EMT: epithelial-mesenchymal transition

CT: critical threshold

Author Contribution Statement

All authors had substantial contributions for conception, design, acquisition of data, analysis, interpretation of data, the drafting of the manuscript and critical revision and final approval for its intellectual content.

Acknowledgements

Ethics approval

The current study was authorized by Research Ethics Committee at Faculty of dentistry, October 6 University (#RECO6U/15-2022) and informed consents were obtained from all donors after explaining the research study and procedure. It is not a part of a student thesis.

Availability of data

The datasets generated during and/or analyzed during the current study are available from the corresponding author on reasonable request.

Conflict of interest

The authors had no conflict of interest concerning the topic under consideration in this article.

References

Ahmadi M, Rezaie J (2020). Tumor cells derived exosomes as angiogenenic agents: possible therapeutic implications. *J Transl Med*, **18**, 249.

Armstrong JP, Holme MN, Stevens MM (2017). Re-engineering extracellular vesicles as smart nanoscale therapeutics. *ACS Nano*, **11**, 69-83.
Cahill EF, Kennelly H, Carty F, Mahon BP, English K (2016). Hepatocyte Growth Factor Is Required for Mesenchymal Stromal Cell Protection Against Bleomycin-Induced Pulmonary Fibrosis. *Stem Cells Transl Med*, **5**, 1307-18.
Chen L, Qian X, Wang Z, Zhou X (2021). The HOTAIR lncRNA: A remarkable oncogenic promoter in human cancer metastasis. *Oncol Lett*, **21**, 1-8.
Cohen O, Betzer O, Elmaliach-Pnini N, et al (2021). 'Golden' exosomes as delivery vehicles to target tumors and overcome intratumoral barriers: in vivo tracking in a model for head and neck cancer. *Biomater Sci*, **9**, 2103-114.
Costa DL, Amaral EP, Andrade BB, Sher A (2020). Modulation of Inflammation and Immune Responses by Heme Oxygenase-1: Implications for Infection with Intracellular Pathogens. *Antioxidants (Basel)*, **9**, 1205.
Coyte A, Morrison DS, McLoone P (2014). Second primary cancer risk - the impact of applying different definitions of multiple primaries: results from a retrospective population-based cancer registry study. *BMC Cancer*, **14**, 1-11.
Dong L, Pu Y, Zhang L, et al (2018). Human umbilical cord mesenchymal stem cell-derived extracellular vesicles promote lung adenocarcinoma growth by transferring miR-410 article. *Cell Death Dis*, **9**, 1– 13.
Gauthaman K, Fong CY, Suganya CA, et al (2012). Extra-embryonic human Wharton's jelly stem cells do not induce tumorigenesis, unlike human embryonic stem cells. *Reprod Biomed Online*, **4**, 235-46.
Gibb EA, Enfield KS, Stewart GL, et al (2011). Long non-coding RNAs are expressed in oral mucosa and altered in oral premalignant lesions. *Oral Oncol*, **47**, 1055-61.
Han T-S, Hur K, Cho H-S, Ban HS (2020). Epigenetic associations between lncRNA/circRNA and miRNA in hepatocellular carcinoma. Cancers, 12(9):1-17.
He Z, Li W, Zheng T, Liu D, Zhao S (2020). Human umbilical cord mesenchymal stem cells-derived exosomes deliver microRNA-375 to downregulate ENAH and thus retard esophageal squamous cell carcinoma progression. *J Exp Clin Cancer Res*, **39**, 140.
Jabbari N, Karimipour M, Khaksar M, et al (2020b). Tumor-derived extracellular vesicles: insights into bystander effects of exosomes after irradiation. *Lasers Med Sci*, **35**, 531–45.
J O'Loughlin A, A Woffindale C, JA Wood M (2012). Exosomes and the emerging field of exosome-based gene therapy. *Curr Gene Ther*, **12**, 262-74.
Kalluri R (2016). The biology and function of exosomes in cancer. *JCI*, **126**, 1208-15.
Katakowski M, Buller B, Zheng X, et al (2013). Exosomes from marrow stromal cells expressing miR-146b inhibit glioma growth. *Cancer Lett*, **335**, 201-4.
Kolenda T, Guglas K, Ryś M, et al (2017). Biological role of long non-coding RNA in head and neck cancers. *Rep Pract Oncol Radiother*, **22**, 378-88.
Lee SS, Yang SF, Tsai CH, et al (2008). Upregulation of heme oxygenase-1 expression in areca-quid-chewing-associated oral squamous cell carcinoma. *J Formos Med Assoc*, **107**, 355-63.
Lei C-S, Kung H-J, Shih J-W (2021). Long non-coding rnas as functional codes for oral cancer: translational potential, progress and promises. *Int J Mol Sci*, **22**, 1-33.
Li R, Chen C, Zheng R, et al (2019). Influences of hucMSC-exosomes on VEGF and BMP-2 expression in SNFH rats. *Eur Rev Med Pharmacol Sci*, **23**, 2935– 43.
Li X, Liu L, Yang J, et al (2016). Exosome Derived From Human Umbilical Cord Mesenchymal Stem Cell Mediates MiR-181c Attenuating Burn-induced Excessive Inflammation. *EBio Med*, **8**, 72-82.
Liew LC, Katsuda T, Gailhouste L, Nakagama H, Ochiya T (2017). Mesenchymal stem cell-derived extracellular vesicles: a glimmer of hope in treating Alzheimer's disease. *Int Immunol*, **29**, 11-9.
Logan CV, Szabadkai G, Sharpe JA, et al (2014). Loss-of-function mutations in MICU1 cause a brain and muscle disorder linked to primary alterations in mitochondrial calcium signaling. *Nat Genet*, **46**, 188-93.
Lu MY, Liao YW, Chen PY, et al (2017). Targeting LncRNA HOTAIR suppresses cancer stemness and metastasis in oral carcinomas stem cells through modulation of EMT. *Oncotarget*, **8**, 98542-52.
Lu Y, Zheng Z, Yuan Y, et al (2021). The Emerging Role of Exosomes in Oral Squamous Cell Carcinoma. *Front Cell Dev Biol*, **9**, 1-13.
Matsuoka Y, Yoshida R, Kawahara K, et al (2022). The antioxidative stress regulator Nrf2 potentiates radioresistance of oral squamous cell carcinoma accompanied with metabolic modulation. *Lab Invest*, **102**, 896-907.
Nishiyama K, Maruyama R, Niinuma T, et al (2018). Screening for long noncoding RNAs associated with oral squamous cell carcinoma reveals the potentially oncogenic actions of DLEU1. *Cell Death Dis*, **9**, 826.
Pourhanifeh MH, Mahjoubin-Tehran M, Shafiee A, et al (2020). MicroRNAs and exosomes: small molecules with big actions in multiple myeloma pathogenesis. *Iubmb Life*, **72**, 314–33.
Priglinger E, Strasser J, Buchroithner B, et al (2021). Label-free characterization of an extracellular vesicle-based therapeutic. *J Extracell.Vesicles*, **10**, e12156.
Qiu L, Wang J, Chen M, Chen F, Tu W (2020). Exosomal microRNA 146a derived from mesenchymal stem cells increases the sensitivity of ovarian cancer cells to docetaxel and taxane via a LAMC2 mediated PI3K/Akt axis. *Int J Mol Med*, **46**, 609-20.
Sabry D, Mohamed A, Monir M, Ibrahim HA (2019). The effect of mesenchymal stem cells derived microvesicles on the treatment of experimental CCL4 induced liver fibrosis in rats. *Int J Stem Cells*, **12**, 400.
Shinagawa K, Yanamoto S, Naruse T, et al (2017). Clinical roles of interleukin-6 and STAT3 in oral squamous cell carcinoma. *Pathol Oncol Res*, **23**, 425-31.
Singh NP, McCoy MT, Tice RR, Schneider EL (1988). A simple technique for quantitation of low levels of DNA damage in individual cells. *Exp Cell Res*, **175**, 184-91.
Tang Q, Hann S (2018): HOTAIR: An Oncogenic Long Non-Coding RNA in Human Cancer. *Cell Physiol Biochem*, **47**, 893-913.
Théry C, Witwer KW, Aikawa E, et al (2018). Minimal information for studies of extracellular vesicles. *J Extracell Vesicles*, **7**, 1535750.
UZ U, Eskiizmir G (2019). Association Between Interleukin-6 and Head and Neck Squamous Cell Carcinoma: A Systematic Review. *Clin Exp Otorhinolaryngol*, **14**, 50-60.
Vakhshiteh F, Atyabi F, Ostad S (2019). Mesenchymal stem cell exosomes: a two-edged sword in cancer therapy. *Int J Nanomedicine*, **14**, 2847– 59.
Weng Z, Zhang B, Wu C, et al (2021). Therapeutic roles of mesenchymal stem cell-derived extracellular vesicles in cancer. *J Hematol Oncol*, **14**, 1-22
Weiss ML, Medicetty S, Bledsoe AR, et al (2006). Human umbilical cord matrix stem cells: preliminary characterization and effect of transplantation in a rodent model of Parkinson's disease. *Stem Cells*, **24**, 781-92.
Weiss ML, Anderson C, Medicetty S, et al (2008). Immune properties of human umbilical cord Wharton's jelly-derived

cells. *Stem Cells*, **26**, 2865-74.
Wu Y, Liu J, Zheng Y, et al (2014). Suppressed expression of long non-coding RNA HOTAIR inhibits proliferation and tumourigenicity of renal carcinoma cells. *Tumour Biol*, **35**, 11887-894.
Wu J, Xie H (2015). Expression of long noncoding RNA-HOX transcript antisense intergenic RNA in oral squamous cell carcinoma and effect on cell growth. *Tumor Biol*, **36**, 8573–8.
Wu Y, Zhang L, Zhang L, et al (2015). Long non-coding RNA HOTAIR promotes tumor cell invasion and metastasis by recruiting EZH2 and repressing E-cadherin in oral squamous cell carcinoma. *Int J Oncol*, **46**, 2586–94.
Xiang E, Han B, Zhang Q, et al (2020). Human umbilical cord-derived mesenchymal stem cells prevent the progression of early diabetic nephropathy through inhibiting inflammation and fibrosis. *Stem Cell Res Ther*, **11**, 336.
Xie Q, Liu R, Jiang J, et al (2020). What is the impact of human umbilical cord mesenchymal stem cell transplantation on clinical treatment?. *Stem Cell Res Ther*, **11**, 519.
Yeo RW, Lai RC, Zhang B, et al (2013). Mesenchymal stem cell: an efficient mass producer of exosomes for drug delivery. *Adv Drug Deliv Rev*, **65**, 336-41.
Yin K, Wang S, Zhao RC (2019). Exosomes from mesenchymal stem/stromal cells: a new therapeutic paradigm. *Biomark Res*, **7**, 1-8.
Yuan Y, Zhou C, Chen X, et al (2018). Suppression of tumor cell proliferation and migration by human umbilical cord mesenchymal stem cells: A possible role for apoptosis and Wnt signaling. *Oncol Lett*, **15**, 8536-44.
Yuan L, Liu Y, Qu Y, Liu L, Li H (2019). Exosomes Derived from MicroRNA-148b-3p-Overexpressing Human Umbilical Cord Mesenchymal Stem Cells Restrain Breast Cancer Progression. *Front Oncol*, **22**, 1076.
Zamani H, Karami F, Mehdizadeh M, Baakhlag S, Zamani M (2022). Long Term Culture of Mesenchymal Stem Cells: No Evidence of Chromosomal Instability. *APJCB*, **7**, 349-53.
Zanoni DK, Montero PH, Migliacci JC, et al (2019). Survival outcomes after treatment of cancer of the oral cavity (1985-2015). *Oral Oncol*, **90**, 115-21.
Zhao X, Wu X, Qian M,et al (2018). Knockdown of TGF-β1 expression in human umbilical cord mesenchymal stem cells reverts their exosome-mediated EMT promoting effect on lung cancer cells. *Cancer Lett*, **428**, 34– 44.
Zhang B, Yin Y, Lai RC, et al (2014). Mesenchymal stem cells secrete immunologically active exosomes. *Stem cells Dev*, **23**, 1233-44.
Zhang B, Shen L, Shi H, et al (2016). Exosomes from Human Umbilical Cord Mesenchymal Stem Cells: Identification, Purification, and Biological Characteristics. *Stem Cells Int*, **2016**, 1-11.
Zhou S, Ye W, Shao Q, Zhang M, Liang J (2013). Nrf2 is a potential therapeutic target inradioresistance in human cancer. *Crit Rev Oncol Hematol*, **88**, 706–15.
Zhu Z, Zhang Y, Zhang H, et al (2019). Exosome derived from human umbilical cord mesenchymal stem cells accelerate growth of VK2 vaginal epithelial cells through MicroRNAs in vitro. *Hum Reprod*, **1**, 248– 60.

This work is licensed under a Creative Commons Attribution-Non Commercial 4.0 International License.